IEEE Access
Multidisciplinary | Rapid Review | Open Access Journal

Received February 11, 2020, accepted February 24, 2020, date of publication March 16, 2020, date of current version March 26, 2020.

Digital Object Identifier 10.1109/ACCESS.2020.2980946

Effects of Temperature Gradient on Electrical Tree Growth and Partial Discharge in Silicone Rubber Under AC Voltage

BOXUE DU[1], (Senior Member, IEEE), TINGTING MA[1], JINGANG SU[2], (Member, IEEE), MENG TIAN[1], TAO HAN[1], (Member, IEEE), AND XIAOXIAO KONG[1]

[1]Key Laboratory of Smart Grid of Education Ministry, School of Electrical and Information Engineering, Tianjin University, Tianjin 300072, China
[2]State Grid Hebei Electric Power Research Institute, Shijiazhuang 050021, China

Corresponding author: Tao Han (hant@tju.edu.cn)

This work was supported by the Chinese National Natural Science Foundation under Grant 51537008, Grant U1966203, and Grant 51707132.

ABSTRACT The Joule heat produced by the current in conductor decreases in the radial direction, producing a temperature gradient in the insulation. This existing temperature gradient can affect the electrical tree phenomenon in insulation materials because of the temperature dependence of insulation material, charge migration and tree growth. Different temperature gradients were obtained by controlling the temperature of high voltage (HV) and ground electrode (GD) sides. The electrical tree was recorded by a microscope, while the partial discharge (PD) was observed simultaneously. For better understanding the effects of the temperature gradient on electrical tree inception, the trap distribution in silicone rubber (SIR) with different temperature was analyzed by isothermal discharge current (IDC) method. With the fixed temperature in HV or GD side, it was found that the electrical tree inception voltage decreased linearly with increasing temperature in either side. The IDC results indicate that the increasing temperature contributes to the de-trapping of charges and lowers the inception voltage. Besides, the electrical tree length and accumulated damage gradually increase with the temperature gradient. The observed PD amplitude and quantity also increase with the temperature gradient, which facilitates the growth of electrical trees. These results indicate that the tree growth is promoted with an increase in the temperature gradient of the cable insulation, posing a threat to the safety of the cable system.

INDEX TERMS AC plastic cable, cable accessories, silicone rubber, electrical tree, temperature gradient, tree inception, growth characteristics, partial discharge.

I. INTRODUCTION

Cable accessories are the weak points in cable operation because of the nonuniform electric field distribution caused by their multilayer insulation structure [1], [2]. Silicone rubber (SIR) is widely used in the main insulation of high-voltage AC cable accessories [3]–[6]. The temperature gradient is formed by Joule heating due to the inner current during the cable operation, which will change the electrical properties of SIR in the radial direction [7]–[9].

Electrical tree, which refers to the local breakdown caused by the local electric field concentration and the dendritic destruction channels generated by this field, is an insulating aging phenomenon in polymers and has been found to be an important factor for the aging of cable accessories [10]–[15]. It is known that the temperature will affect both the electrical tree inception and growth processes [16]–[20]. The electrical tree inception is related to the electron injection-extraction process and charge transport [21], [22], and the growth characteristics are determined by partial discharge (PD) and space charge accumulation [23], [24]. The charge behavior of insulation makes the distortion of the electric field inside cable accessories more severe, readily leading to insulation degradation [17], [23], [25].

To date, it has been found that temperature affects the electrical tree inception. In [26], the average tree inception

The associate editor coordinating the review of this manuscript and approving it for publication was Md. Moinul Hossain.

voltage was found to decrease exponentially with increased temperature, changing by 42%. Single-branch trees and multiple-branch trees were observed. The probability of the generation of multiple-branch trees decreased with increasing temperature. In [27], a relationship between the electrical tree growth process and PD was found. Different tree structures and growth stages are associated with different PD characteristics. In [28], the behavior of space charge under a temperature gradient was studied. It was found that different temperature conditions applied to the electrodes have a strong effect on distribution of space charge. However, the effects of charge transport in the presence of a temperature gradient on electrical tree growth and PD characteristics have only rarely been investigated.

In this paper, inception characteristics, morphology and accumulated damage of the electrical tree were analyzed under the combination of an AC voltage and a temperature gradient. The trap distribution was tested at different temperatures. The relationship between the electrical tree inception and charge transport process was discussed. A PD detector was employed to record the PD characteristics during the electrical tree growth process. The effects of the temperature gradient on PD characteristics were discussed based on the experimental results.

II. EXPERIMENTAL SETUP

A. SAMPLE PREPARATION

The SIR used in this experiment was a high-temperature-vulcanized (HTV) SIR. The raw material in the preparation of SIR samples was 110-2 raw rubber. Raw rubber and mass fraction of 1% vulcanizing agent were evenly mixed. The mixed raw rubber was placed in a 3 mm thick mold of a hot press vulcanizing machine. The vulcanization process at a temperature of 170 °C and a pressure of 20 MPa was carried out for 15 min. After the sample was cooled to room temperature, it was taken out and cut into a square sample with the dimension of 15 mm × 15 mm. A steel needle with a tip radius of 3 μm was inserted into the center of the SIR sample, and the needle tip was placed 2 mm away from the bottom surface. The prepared samples were placed in a thermal box for secondary vulcanization carried out at 0.1 MPa and 165 °C for 24 hours.

B. EXPERIMENTAL SETUP

The experimental setup consists of the following four parts: an electrical tree observation system, a PD acquisition system, a temperature controller and a high voltage AC source. The experimental setup is shown in Figure 1. The SIR sample was placed between the needle-plate electrodes. The needle electrode was used to apply an AC voltage, and the plate electrode was the ground electrode. The ground electrode was in close contact with the bottom surface of the sample. The temperature controller includes a temperature gradient control system and heating unit. The heating tapes of the heating unit were placed on the needle electrode and the ground electrode. To collect the image of the electrical tree growth process, the heating tape at the needle electrode side was placed 1 mm above the tip of the needle. The temperature controller (XY-WT01) has a temperature control range of -50 to 110 °C and the error range of ±0.1 °C. It can maintain a constant temperature at the preset value. If the heating tapes temperature exceed the preset value, the cooling system in the temperature gradient control system will quickly cool the heating tapes. We call the heating tape temperature near the needle tip as the high-voltage-side temperature, and the heating tape temperature of the ground electrode as the ground-side temperature. To ensure the accuracy of the experimental temperature, the samples were preheated for 10 min prior to each experiment. The high-voltage-side temperature was fixed to 30, 60 and 90 °C. At each high-voltage-side temperature, the ground-side temperature was changed in the steps of 10 °C in the range of 30-90 °C to form the temperature gradient. In addition, the ground-side temperature was fixed to 30, 60 and 90 °C, and the high- voltage-side was varied in the same way within the range of 30-90 °C. Table 1 shows the conditions of the fixed high-voltage-side temperature and changing ground side temperature used in the experiments. The method of fixing the ground-side temperature and changing the high-voltage-side temperature is as mentioned above. To reduce the experimental error, 20 samples were tested for each temperature gradient.

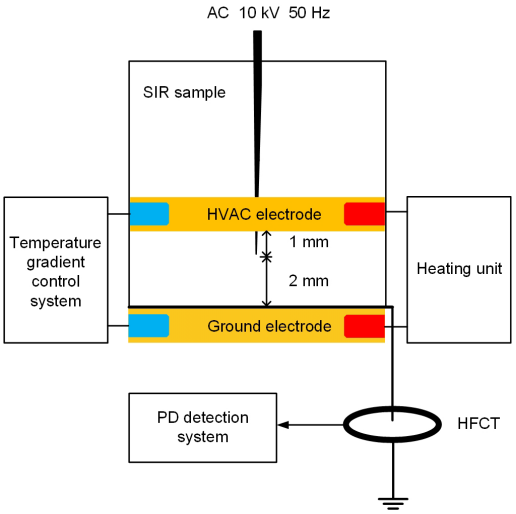

FIGURE 1. Experimental setup for electrical tree of SIR with the ΔT.

The typical electrical treeing experiment and PD measurement were carried out simultaneously. A high-frequency current transformer (HFCT) was installed on the ground cable to detect the PD signals. A PD detection system (Techimp PDCheck) was employed to record the PD signals detected by HFCT. The PD test setup diagram and more details can be found in [25]. The AC voltage has an amplitude of 10 kV and a frequency of 50 Hz.

ΔT refers to the temperature gradient, and its value was recorded as the temperature difference between the

TABLE 1. Electrical tree test groups in experiment.

High voltage side temperature (°C)	Ground side temperature (°C)	Temperature gradient (°C)
30	30	Δ0
	40	Δ−10
	50	Δ−20
	60	Δ−30
	70	Δ−40
	80	Δ−50
	90	Δ−60
60	30	Δ+30
	40	Δ+20
	50	Δ+10
	60	Δ0
	70	Δ−10
	80	Δ−20
	90	Δ−30
90	30	Δ+60
	40	Δ+50
	50	Δ+40
	60	Δ+30
	70	Δ+20
	80	Δ+10
	90	Δ0

high-voltage side and the ground side, as given by:

$$\Delta T = T_{HV} - T_{GD} \tag{1}$$

where T_{HV} is the temperature of the high-voltage side and T_{GD} is the temperature of the ground side. When ΔT is greater than zero, it is referred to as positive ΔT. When ΔT is less than zero, it is referred to as negative ΔT. The symbol ''HV'' represents the high-voltage electrode, and ''GD'' represents the ground electrode.

III. RESULTS AND DISCUSSION

A. FIXED TEMPERATURE IN HV SIDE

In this experiment, the tree inception voltages were measured with the constant voltage rising speed, and the rate of the voltage increase was 0.5 kV/ 30 s, the same as our previous works [14]. The voltage increase speed will affect the experimental results in each experiment. The method to reduce the error of experimental results is to keep the same voltage rising speed. The voltage at the time when the length of the electrical tree was observed to reach 20 μm was recorded. To reduce the experimental error, 20 groups were recorded, and the average electrical tree inception voltage was calculated under a ΔT. The results are shown in Figure 2, and it is observed that the tree inception voltage decreases linearly as the GD side temperature increases at each HV side temperature. At the same GD side temperature, a higher HV side temperature shows a lower inception voltage. A partial temperature rise will make the insulation more vulnerable to damage and trigger an electrical tree.

The electrical tree structures found in these experiments mainly include the branch tree, bush-branch tree and bush tree. In this work, the tree structure at 5 min was analyzed, where the AC voltage has an amplitude of 10 kV and a frequency of 50 Hz, as shown in Figure 3. At Δ0, the black

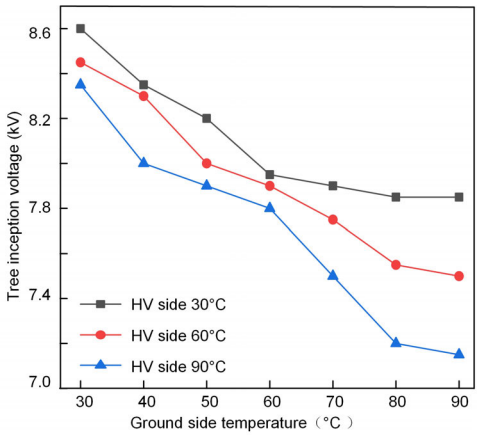

FIGURE 2. Relationship between the tree inception voltage and the ΔT.

tree channels increase with an increase in the temperature, and the tree structure changes from the sparse branch tree to the bush-branch tree, as shown in Figure 3a1 to 3b1. At the HV side temperature of 30 °C, as shown in Figure 3a, the electrical tree structure is that of a sparse branch tree at Δ0. With the increase in Δ T, the tree structure changes from the sparse branch tree to bush-branch tree. Under negative ΔT, these trees exhibit an arc-like outline, as shown in Figure 3a3. At the HV side temperature of 60 °C, as shown in Figure 3b, with the increase in ΔT, the black areas of electrical trees increase. Furthermore, the electrical tree has more black channels under the positive ΔT than the negative ΔT. At the HV side temperature of 90 °C, as shown in Figure 3c. When the ΔT increases, the electrical tree structures are all bush-branch tree, and the channels of the tree branch become denser. The electrical tree length grows considerably more in the longitudinal direction than in the lateral direction, and the tree structure outline tends to become triangular. As shown in Figure 3c3, under positive ΔT, the triangular outline of these trees can be observed at large ΔT.

Figure 4 shows the tree length for 30 min. The tree length is defined as the longest distance from the needle tip to the tree tip in the vertical direction. With an increase in ΔT, the tree length gradually increases. When the HV side is 30 °C, as the ΔT increases, the length rises to approximately 27%. When the HV side is 90 °C, the tree length rises to approximately 59%, and the tree length variation achieves the largest range as the ΔT increases. The results show that the partial temperature rise in the inner insulation is likely to accelerate the growth of electrical trees.

In the research on electrical tree, the accumulated damage (AD) is usually employed to analyze the destroyed area caused by tree, which is usually calculated by summing the pixel number in the tree area. The obtained results for the accumulated damage after 30 min are shown in Figure 5. At the HV side temperature of 30, 60 and 90 °C, the accumulated damage increases monotonically with an increase in ΔT. At the HV side temperature of 30 °C, it is observed

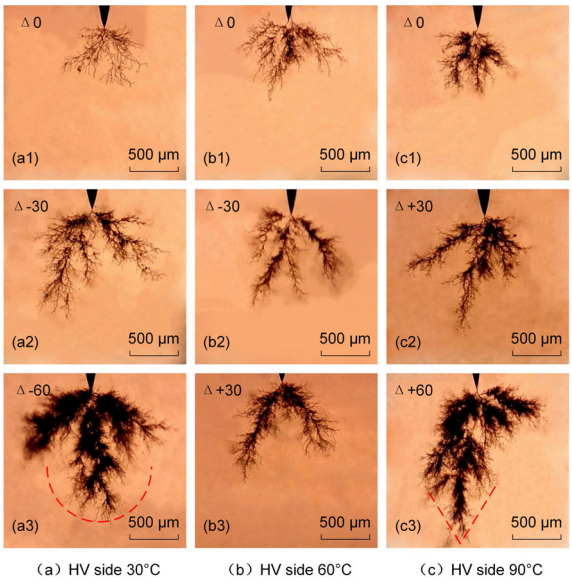

FIGURE 3. Typical tree structure with the ΔT for 5 min.

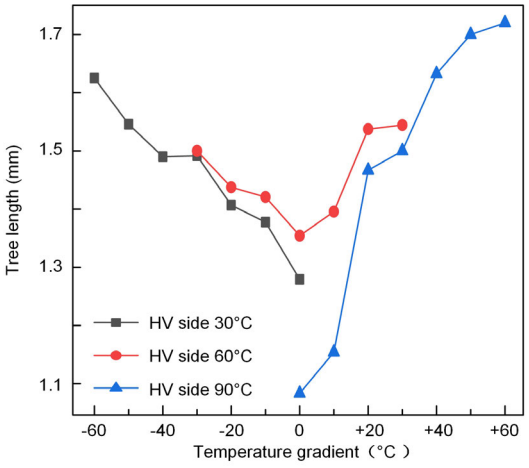

FIGURE 4. Relationship between the tree length and the ΔT.

from Figures 3 and 4 that the tree structure and tree length change significantly with the increase in ΔT. As a result, the largest values of accumulated damage are obtained, as shown in Figure 5. Based on the experimental results, it was found that when the HV side is 90 °C, the accumulated damage variation was less than that when the HV side is 30 °C. At the HV side temperature of 90 °C, the electrical tree structure does not change notably with increasing ΔT, and the main reason for the accumulated damage increase was the electrical tree length. The difference in the magnitude of the accumulated damage is the result of the different degrees of influence on the tree length and structure. Accumulated damage is the result of the changing electrical tree length and structure. Although both the tree length and accumulated damage increase with ΔT, the shortest tree length in Figure 4 was obtained at the HV side temperature of 90 °C and Δ0.

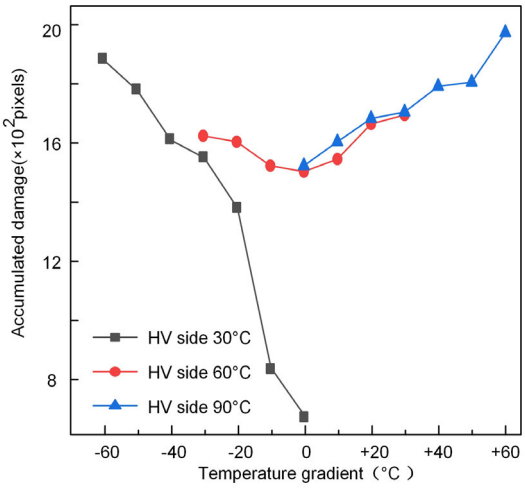

FIGURE 5. Relationship between the accumulated damage and the ΔT.

By contrast, the lowest accumulated damage in Figure 5 was obtained at the HV side temperature of 30 °C and Δ0. When SIR is at a higher temperature, the tree structure is denser, and the structure makes the charges distribution more dispersed in a large number of channels. The electric field formed by the dispersed charges is uniform. The electrical tree length is limited, and accumulated damage only occurs in a spherical area under the uniform electric field.

B. FIXED TEMPERATURE IN GD SIDE

Figure 6 shows the tree inception voltages obtained under a fixed temperature in the GD side and changing temperature in the high-voltage side. The method for calculating the tree voltage is the same as described above. As the high-voltage-side temperature increases, the tree inception voltages show a downward trend. Compared with Figure 2, it is found that the distance between the tree inception voltage curves in Figure 6 is large, and the three curves in Figure 6 are steep.

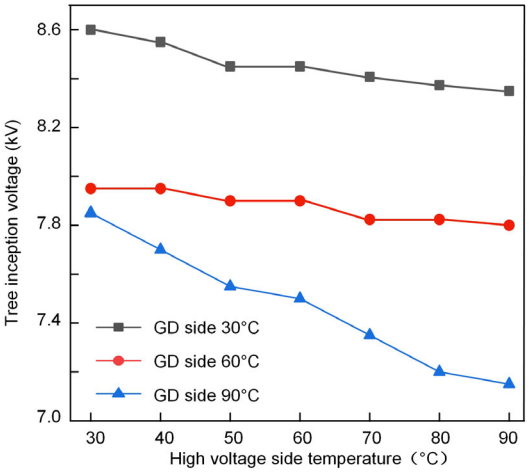

FIGURE 6. Relationship between the tree inception voltage and the ΔT.

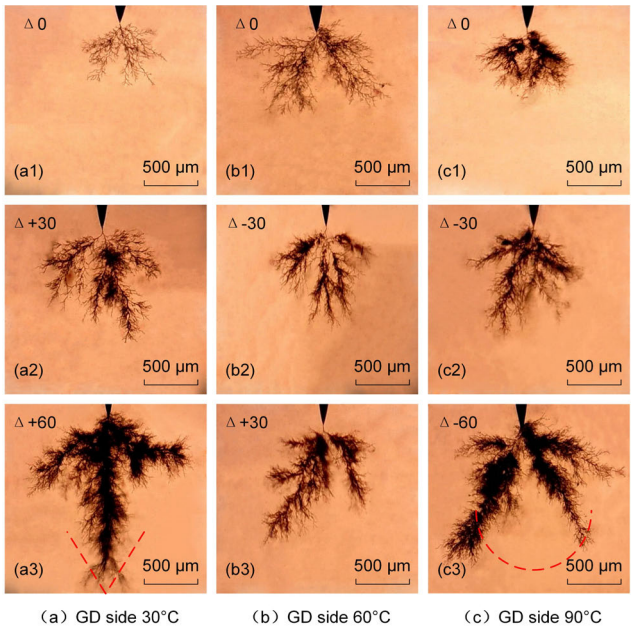

FIGURE 7. Typical tree structure with the ΔT for 5 min.

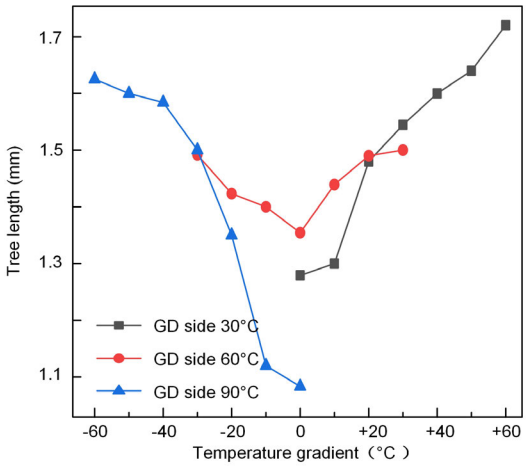

FIGURE 8. Relationship between the tree length and the ΔT.

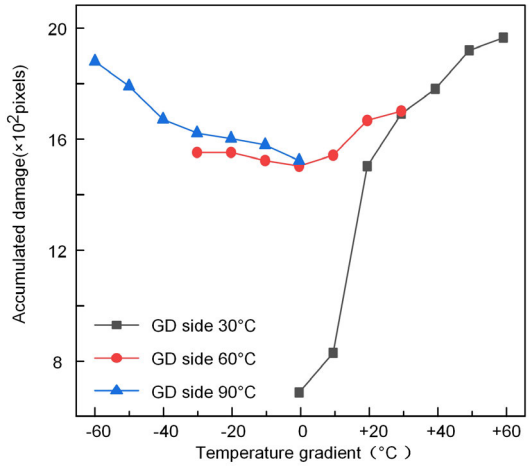

FIGURE 9. Relationship between the accumulated damage and the ΔT.

This result shows that the change of the GD side temperature has a strong effect on the tree inception voltage.

Figure 7 shows the typical tree structures with ΔT for 5 min. For the GD side temperature of 30 °C, the branch and bush-branch trees are observed in Figure 7a, where the branch tree is at Δ0. With an increase in ΔT, the electrical tree channels tend to be darker. The outline of these tree tends to become triangular. The tree outline in Figure 3a3 is the opposite of that in Figure 7a3. For the GD side temperature of 60 °C, the color of the electrical tree channels deepened with increased ΔT. For the GD side temperature of 90 °C, it is observed in Figure 7c that the trees are dark and are found in a bush-branch structure. The outline of these trees tends to be arc with an increase in ΔT, as shown by the red line in Figure 7c3. The temperature rise of the GD side makes the tree outline tend to become arc-like. The temperature rise of the HV side makes the tree outline tend to become triangular.

Figure 8 shows the relationship between the tree length and ΔT under a fixed temperature in the GD side for 30 min. With an increase in ΔT, the tree length gradually increases. The electrical tree length is longer under positive ΔT. This trend is approximately the same as that shown in Figure 4. An examination of Figure 4 shows that for the HV side temperature of 90 °C, the curve rises from the lowest point to the highest point as the ΔT increases. By contrast, as shown in Figure 8, for the GD side temperature of 90 °C, the highest point is not on this curve. This finding indicates that with the temperature rise of the GD side, a certain limit on the tree length is reached. This phenomenon may be due to the arc shape of the tree outline near the GD side. Of the two observed outlines, namely, triangle and arc, the former is more likely to cause the charges to concentrate at the tip of the electrical tree. The arc tree outline makes the electric field at the tip of the electrical tree more uniform. Nonuniform electric field causes by charge accumulation, which promotes electrical tree growth. The length of the electrical tree is an important parameter for the appearance of insulation damage. When the electrical tree is long enough, it will give rise to an insulation breakdown. The results show that the temperature rise in the inner insulation is likely to pose a risk of insulation degradation and failure.

The results for accumulated damage after 30 min are shown in Figure 9. At the GD side temperatures of 30, 60 and 90 °C, the accumulated damage increases monotonically with rising ΔT. The accumulated damage curve is steep at the GD side temperature of 30 °C. The curve changes gently at the GD side temperatures of 60 and 90 °C. Compared with Figure 5, for the GD or HV side temperatures of 30 °C, the variation range is large. For the GD or HV side temperatures of 90 °C, the curve changes gently. The tree structure and accumulated damage depend on the highest temperature of the electrode such that if the highest temperature is constant, the tree

structure and accumulated damage do not change much with increasing ΔT.

C. TRAP DISTRIBUTION

The isothermal discharge current (IDC) is a method for studying the trap energy level and the trap density distribution in the insulation by measuring the change in the discharge current. The HTV SIR raw materials and preparation method are the same as the Section 2.1 for the IDC test samples, where the thickness of the sample is 300 μm. The IDC test setup diagram and more details can be found in [29]–[31]. The working principle of the experiment is to polarize the insulation at a constant temperature by injecting charges into the volume and forming space charges. The trap distribution characteristic is obtained by measuring the external current in the charge detrapping process when the insulation is depolarized [32]. Based on this method, the trap distribution characteristics at 30, 50, 70 and 90 °C were tested. The trap density and energy levels in the polymer are important parameters for the injection-extraction process and the space charge accumulation.

The relationship between the trap density and energy level is described in detail in [33]–[35] and is given by

$$\frac{N_t(E)}{E_t} = \frac{I}{\frac{eLSK_BT}{2t}K_BT\ln(\nu t)} \tag{2}$$

where $Nt(E)$ is the trap density in $\mathrm{eV}^{-1}\mathrm{m}^{-3}$, Et is the trap energy in eV, I is the external current, e is the elementary charge in C, L is the sample thickness in m, S is the electrode area in m^2, K_B is the Boltzmann constant, T is the temperature in K, t is the time in s, and ν is the escape attempt frequency in s^{-1}. It should be noted that ν can be expressed by the equation:

$$\nu = \frac{K_BT}{h} \tag{3}$$

where h is the Planck constant in J·s.

Figure 10 shows the trap distribution of the ambient temperature measured by the IDC method under the negative DC voltage. It is observed that there are two distinct peaks in the trap energy distribution at each temperature. The trap distribution can be regarded as a combination of two curves representing the distributions of shallow traps and deep traps, respectively. The ordinate axis represents the trap density, and the abscissa axis represents the trap energy level. It is generally believed that the trap density is determined by the material. In the same sample, the difference in shallow traps is mainly related to the time of the switching action during the experiment because it is determined by the beginning part of data. As the temperature increases, the central energy level of the deep trap distribution keeps rising. High temperature enables the electrons to detrap with a high thermal kinetic energy. This shows that high temperature causes electrons to escape from the trap with high energy levels. These detrapped electrons contribute to the current in the external circuit.

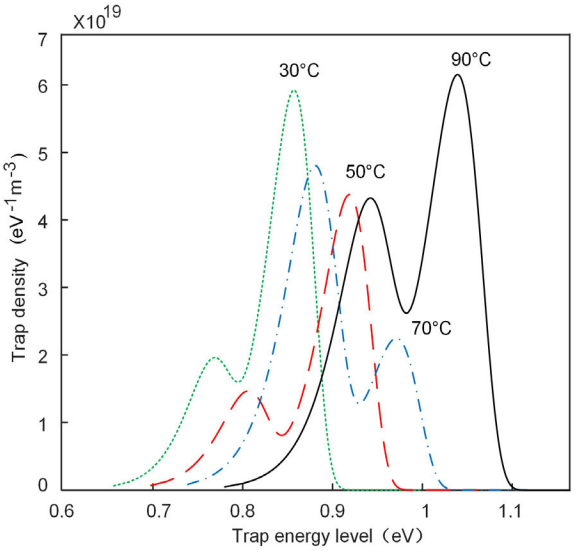

FIGURE 10. Trap distribution at ambient temperature measured by the IDC method.

The charge behavior and SIR material property under the ΔT influenced by trap distribution are associated with the tree inception voltages. A discharge may occur in the low-density region and generate an initial electrical tree channel when the low-density region is sufficiently large. The fracture of the SIR molecular chains will create low density regions. Hence, the breaking of the SIR molecular chains is the key for triggering the electrical tree. The electrons in the traps can easily obtain energy due to thermal stimulation [36]. These electrons escape from the trap and become hot electrons. The high temperature will trigger more hot electrons, causing the SIR molecular chains to break [37]. The high number of hot electrons produced by thermal stimulation is the main reason for the decrease of the tree inception voltage as the GD temperature rises with each HV side temperature, as shown in Figure 2. The increasing number of injected charges is one of the reasons for the lower tree inception voltage as the HV temperature rises, as shown in Figure 6. The injection current occurring in the interface between the high-voltage electrode and the SIR sample can be obtained by the Schottky formula [37], [38]. The increase in the HV side temperature leads to a decrease in the Schottky barrier and increases the injected charge.

From the perspective of material properties, the SIR material absorbs heat in the temperature range of 30-90 °C, and the thermal motion of the SIR molecular chains gradually increases with increasing temperature. The rising temperature causes greater partial relaxation of the SIR molecular chains [37], [39]. The increase in the carrier mobility increases the probability of breaking the relaxed SIR molecular chains. Therefore, the tree inception voltages drop with the increase in either the HV or the GD side temperature. The larger interval of the three curves in Figure 6 and the three steep curves in Figure 2 indicates that the hot electrons have a stronger effect on the inception voltage.

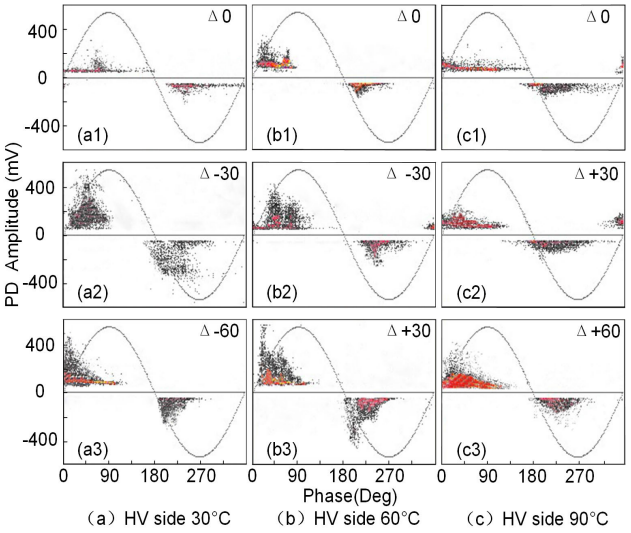

FIGURE 11. PRPD under ΔT at 5 min.

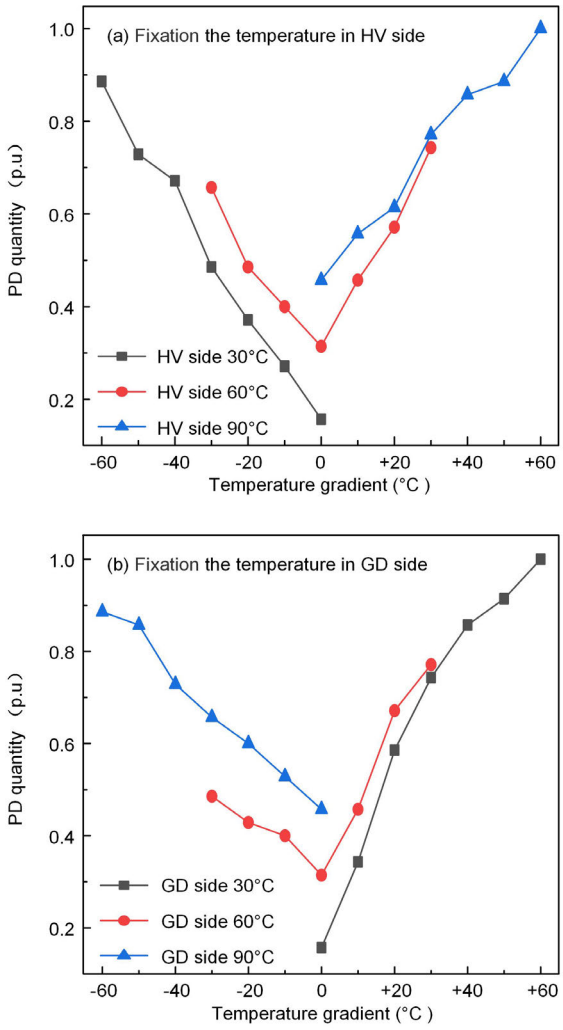

FIGURE 12. Relationship between the discharge quantity and the ΔT.

D. PD CHARACTERISTICS

The PD inside the tube is one of the main accelerating factors of tree growth [40]. The PD in the tree channels can be caused by the space charge accumulation in the tube [41] and SIR near the tube. The space charge accumulation generates an electric field, leading to a partial breakdown, and a tree channel will be generated when the local field reaches a certain level. To analyze the PD characteristics, phase resolved partial discharge (PRPD) and PD quantity measurements at 5 min after the voltage application were employed here.

The PRPD spectrum of the discharge amplitude of the nine kinds of PD signals obtained in the experiment is shown in Figure 11. With an increase in ΔT, the PD amplitude gradually increases. For the HV side temperature of 30 °C, the PD amplitude is high, and a low number of discharges are observed. For the HV side temperature of 60 °C, PD center is found to be dispersed, and the position of the PD center does not change significantly with an increase in ΔT. For the HV side temperature of 90 °C, the discharge amplitude is lower than that for the HV side temperatures of 30 and 60 °C.

PD quantity was obtained under the ΔT. The PD quantity is normalized based on their peak quantity prior to analysis. The results are shown in Figure 12, and it is observed that with an increase in ΔT, the PD quantity gradually increases. Considering these results together with the growth characteristics of electrical trees, it is concluded that PD quantity corresponds to the length and cumulative damage of trees.

Space charges will be injected into SIR following the Schottky-Richardson injection [41], [42]. The increase in the temperature is also likely to enhance the charge accumulation at the tree tips [43]. In addition, the increase in mobility is more pronounced at higher temperatures [36]. Under the positive ΔT, the temperature near needle tip is high. Hence, the space charges will be easily injected in SIR near the tip. This phenomenon promotes electrical tree growth. However, under the negative ΔT, the temperature far from the needle tip is high, and the charge is more likely to escape from the trap and be scattered on the inner wall of the electrical tree channels. In addition, scattered electrical tree channels are easily generated by the relaxation of the SIR molecular chain. Hence, the temperature rise of the HV side makes the tree outline tend to become triangular. The temperature increase of the GD side leads to the tree outline tending to become arc-like.

The local field at the tree boundary is more dependent upon the space charge and its arrangement [43]. The temperature affects the carrier mobility [36]. It is speculated that the space charge accumulation is the result of carrier transport, where the temperature affects the carrier transport and changes the space charge arrangement in electrical tree channels. Electrons are injected from the needle tip, and when the HV side is under high temperature, the injected charges move more quickly and disperse more widely in the tube to form space charge accumulation. Space charge accumulation will give rise to the PD [5], [44]. For the HV side temperature

of 90 °C, the lower discharge amplitude and the larger number of discharges will produce more tiny channels, giving rise to the dense bush-branch electrical tree structure, as shown in Figure 3. For the HV side temperature of 30 °C, the low temperature slows the thermal motion of the charges, leading to greater space charge accumulation in the electrical tree channels and higher discharge amplitude. Therefore, the PD amplitude for the HV side temperature of 90 °C is lower than the HV side temperature of 30 °C. These values reveal that space charge accumulation and charge distribution are affected by the ΔT. A partial black area is appeared at 60 °C and $\Delta 0$ in Figure 3, compared with the electrical tree at 30 °C and $\Delta 0$. A more intense PD may occur in this black area, so the PD amplitude increases. At the HV side temperature of 90 °C, the dispersed space charges are the reason for the reduction of the PD amplitude. With temperature gradient, distribution of space charges around the tree channel tip and migration of space charges will be different and influence the tree structure.

The temperature promotes charges acceleration in the high-temperature region and slows their movement in the low-temperature region. Under positive ΔT, the HV side temperature is higher than the GD side temperature. The electrons with high energy are injected by the needle tip, and the high temperature leads the electrons to move further away from the tip. In addition, the high temperature enhances the Schottky injection and increases carrier mobility at the interface between the needle tip and the SIR material. When the charges move to a position away from the needle tip, the temperature also gradually decreases, and the charge motion slows down to form charge accumulation. The local electric field produced by charge accumulation will trigger the PD and accelerate tree growth. A larger ΔT will give rise to the formation of a more intense PD. The tree length and accumulated damage are increased. Under the negative ΔT, the GD side temperature is high. The tree length growth is mainly affected by the relaxation of the SIR molecular chains and the accelerated charges near the GD side. The thermal motion of the SIR molecular chains makes them easier for them to be broken with the increase in the GD side temperature. On the other hand, the electrons near the ground electrode will accelerate, and the accelerated electrons are more likely to break the SIR molecular chain, forming a low-density region. A discharge may occur in this low-density region. Therefore, the length and accumulated damage of the electrical tree increase under the positive and negative ΔT. This effect explains the increase in PD quantity and amplitude with an increase in ΔT. Higher temperature always has the effect of chain relaxation and carrier acceleration in SIR. However, Schottky injection enhancement near needle tip may cause a slightly larger accumulated damage under positive ΔT. Hence, higher accumulated damage occurs with positive ΔT. Under ΔT, carrier mobility increased with the partial temperature, making an important contribution to the increasing tree length and accumulated damage.

IV. CONCLUSION

In this paper, inception characteristics, morphology and accumulated damage of electrical trees were analyzed under the combination of an AC voltage and a ΔT. The trap distribution was tested at different temperatures. The relationship between electrical tree inception and the charge transport process was discussed. PD detector was employed to record the PD characteristics during the electrical tree growth process. The PD characteristics affected by ΔT were discussed based on the experimental results. The main conclusions are as follows:

1) The tree inception voltage linearly decreases as the GD side temperature increases at each HV side temperature, and the inception voltage decreases linearly with the increasing HV side temperature. The charge behavior and SIR material property under the ΔT influenced by the trap distribution are associated with the tree inception voltages. A partial temperature increase will make the insulation more susceptible to the damaged and trigger the appearance of electrical trees.

2) The temperature rise of the GD side makes the tree outline tend to become arc-like. The temperature rise of the HV side makes the tree outline tend to become triangular. The charge kinetic properties and distribution of space charges around the tree channel tip influenced by temperature may be the main reasons for the change of tree structure.

3) The tree length and accumulated damage gradually increase with ΔT. Under ΔT, carrier mobility increases with the partial temperature, making an important contribution to the increasing tree length and accumulated damage. The increase in ΔT leads to serious deterioration of insulation.

4) The PD amplitude and quantity increase with ΔT. PD quantity corresponds to the tree length and accumulated damage. With an increase in the ΔT, the tree growth deteriorates severely, and it was accompanied by intensive PD activity.

REFERENCES

[1] X. Wang, C. C. Wang, K. Wu, D. M. Tu, S. Liu, and J. K. Peng, "An improved optimal design scheme for high voltage cable accessories," *IEEE Trans. Dielectr. Electr. Insul.*, vol. 21, no. 1, pp. 5–15, Feb. 2014.

[2] J. Li, B. X. Du, and H. Xu, "Suppressing interface charge between LDPE and EPDM for HVDC cable accessory insulation," *IEEE Trans. Dielectr. Electr. Insul.*, vol. 24, no. 3, pp. 1331–1339, Jun. 2017.

[3] B. X. Du, Z. L. Ma, Y. Gao, and T. Han, "Effect of ambient temperature on electrical treeing characteristics in silicone rubber," *IEEE Trans. Dielectr. Electr. Insul.*, vol. 18, no. 2, pp. 401–407, Apr. 2011.

[4] Y. Zhou, Y. Zhang, L. Zhang, D. Guo, X. Zhang, and M. Wang, "Electrical tree initiation of silicone rubber after thermal aging," *IEEE Trans. Dielectr. Electr. Insul.*, vol. 23, no. 2, pp. 748–756, Apr. 2016.

[5] B. X. Du, Z. L. Li, and J. Li, "Effects of direct fluorination on space charge accumulation in HTV silicone rubber," *IEEE Trans. Dielectr. Electr. Insul.*, vol. 23, no. 4, pp. 2353–2360, Aug. 2016.

[6] C. Yuan, C. Xie, L. Li, X. Xu, S. M. Gubanski, Y. Zhou, Q. Li, and J. He, "Space charge behavior in silicone rubber from in-service aged HVDC composite insulators," *IEEE Trans. Dielectr. Electr. Insul.*, vol. 26, no. 3, pp. 843–850, Jun. 2019.

[7] M. Xiao and B. X. Du, "Review of high thermal conductivity polymer dielectrics for electrical insulation," *High Voltage*, vol. 1, no. 1, pp. 34–42, Apr. 2016.

[8] W. Choo, G. Chen, and S. G. Swingler, "Electric field in polymeric cable due to space charge accumulation under DC and temperature gradient," *IEEE Trans. Dielectr. Electr. Insul.*, vol. 18, no. 2, pp. 596–606, Apr. 2011.

[9] D. He, W. Wang, J. Lu, G. Teyssedre, and C. Laurent, "Space charge characteristics of power cables under AC stress and temperature gradients," *IEEE Trans. Dielectr. Electr. Insul.*, vol. 23, no. 4, pp. 2404–2412, Aug. 2016.

[10] I. Iddrissu, H. Zheng, and S. M. Rowland, "DC electrical tree growth in epoxy resin and the influence of the size of inceptive AC trees," *IEEE Trans. Dielectr. Electr. Insul.*, vol. 24, no. 3, pp. 1965–1972, Jun. 2017.

[11] B. X. Du, J. G. Su, and T. Han, "Compressive stress dependence of electrical tree growth characteristics in EPDM," *IEEE Trans. Dielectr. Electr. Insul.*, vol. 25, no. 1, pp. 13–20, Feb. 2018.

[12] D. He, F. Meng, H. Liu, Q. Li, and X. Wang, "The influence mechanism of semiconductive material on space charge accumulation in HVDC cable accessory," *IEEE Trans. Dielectr. Electr. Insul.*, vol. 26, no. 5, pp. 1479–1486, Oct. 2019.

[13] Y. Liu, X. Cao, and G. Chen, "Electrical tree initiation in XLPE cable insulation under constant DC, grounded DC, and at elevated temperature," *IEEE Trans. Dielectr. Electr. Insul.*, vol. 25, no. 6, pp. 2287–2295, Dec. 2018.

[14] B. Du, T. Han, and J. Su, "Electrical tree characteristics in silicone rubber under repetitive pulse voltage," *IEEE Trans. Dielectr. Electr. Insul.*, vol. 22, no. 2, pp. 720–727, Apr. 2015.

[15] N. Rouha and A. Beroual, "Diagnosis of EPDM's aging by electrical trees," *IEEE Trans. Dielectr. Electr. Insul.*, vol. 22, no. 5, pp. 2852–2857, Oct. 2015.

[16] B. X. Du, J. G. Su, and T. Han, "Temperature-dependent electrical tree in silicone rubber under repetitive pulse voltage," *IEEE Trans. Dielectr. Electr. Insul.*, vol. 24, no. 4, pp. 2291–2298, Sep. 2017.

[17] Z. Lei, J. Song, P. Geng, M. Tian, L. Lin, C. Xu, C. Feng, J. Zeng, and Z. Li, "Influence of temperature on dielectric properties of EPR and partial discharge behavior of spherical cavity in EPR insulation," *IEEE Trans. Dielectr. Electr. Insul.*, vol. 22, no. 6, pp. 3488–3497, Dec. 2015.

[18] N. Shimizu and C. Laurent, "Electrical tree initiation," *IEEE Trans. Dielectr. Electr. Insul.*, vol. 5, no. 5, pp. 651–659, Dec. 1998.

[19] T. Han, B. X. Du, Y. Yu, and X. Q. Zhang, "Effect of cryogenic temperature on tree characteristics in silicone Rubber/SiO_2 nanocomposites under repetitive pulse voltage," *IEEE Trans. Appl. Supercond.*, vol. 26, no. 7, pp. 1–4, Oct. 2016.

[20] W. Song, W.-W. Shen, G.-J. Zhang, B.-P. Song, Y. Lang, G.-Q. Su, H.-B. Mu, and J.-B. Deng, "Aging characterization of high temperature vulcanized silicone rubber housing material used for outdoor insulation," *IEEE Trans. Dielectr. Electr. Insul.*, vol. 22, no. 2, pp. 961–969, Apr. 2015.

[21] S. Zhang, Y. Yang, Q. Li, J. Hu, B. Zhang, and J. He, "Different microscopic features of AC and DC electrical trees in insulating polymer," *IEEE Trans. Dielectr. Electr. Insul.*, vol. 25, no. 6, pp. 2259–2265, Dec. 2018.

[22] K. Wu and L. A. Dissado, "Model for electrical tree initiation in epoxy resin," *IEEE Trans. Dielectr. Electr. Insul.*, vol. 12, no. 4, pp. 655–668, Aug. 2005.

[23] A. Cavallini, M. Conti, G. C. Montanari, C. Arlotti, and A. Contin, "PD inference for the early detection of electrical treeing in insulation systems," *IEEE Trans. Dielectr. Electr. Insul.*, vol. 11, no. 4, pp. 724–735, Aug. 2004.

[24] Z. L. Li, B. X. Du, Z. R. Yang, and C. L. Han, "Temperature dependent trap level characteristics of graphene/LDPE nanocomposites," *IEEE Trans. Dielectr. Electr. Insul.*, vol. 25, no. 1, pp. 137–144, Feb. 2018.

[25] M. Liu, Y. Liu, Y. Li, P. Zheng, and H. Rui, "Growth and partial discharge characteristics of electrical tree in XLPE under AC-DC composite voltage," *IEEE Trans. Dielectr. Electr. Insul.*, vol. 24, no. 4, pp. 2282–2290, Sep. 2017.

[26] Y. Zhang, L. Zhang, Y. Zhou, M. Chen, M. Huang, and R. Liu, "Temperature dependence of DC electrical tree initiation in silicone rubber considering defect type and polarity," *IEEE Trans. Dielectr. Electr. Insul.*, vol. 24, no. 5, pp. 2694–2702, Oct. 2017.

[27] I. Iddrissu, S. M. Rowland, H. Zheng, Z. Lv, and R. Schurch, "Electrical tree growth and partial discharge in epoxy resin under combined AC and DC voltage waveforms," *IEEE Trans. Dielectr. Electr. Insul.*, vol. 25, no. 6, pp. 2183–2190, Dec. 2018.

[28] J. Dong, Z. Shao, Y. Wang, Z. Lv, X. Wang, K. Wu, W. Li, and C. Zhang, "Effect of temperature gradient on space charge behavior in epoxy resin and its nanocomposites," *IEEE Trans. Dielectr. Electr. Insul.*, vol. 24, no. 3, pp. 1537–1546, Jun. 2017.

[29] B. X. Du, X. X. Kong, Y. Q. Xing, and J. Li, "Trap distribution of electron beam irradiated epoxy resin under repetitive pulse voltage," *IEEE Trans. Dielectr. Electr. Insul.*, vol. 24, no. 6, pp. 3869–3877, Dec. 2017.

[30] B. X. Du, M. Y. Wang, J. Li, and Y. Q. Xing, "Temperature dependent surface charge and discharge behavior of epoxy/AIN nanocomposites," *IEEE Trans. Dielectr. Electr. Insul.*, vol. 25, no. 4, pp. 1300–1307, Aug. 2018.

[31] B. X. Du, C. Han, Z. Li, and J. Li, "Effect of graphene oxide particles on space charge accumulation in LDPE/GO nanocomposites," *IEEE Trans. Dielectr. Electr. Insul.*, vol. 25, no. 4, pp. 1479–1486, Aug. 2018.

[32] J. Su, B. Du, T. Han, Z. Li, M. Xiao, and J. Li, "Multistep and multiscale electron trapping for high-efficiency modulation of electrical degradation in polymer dielectrics," *J. Phys. Chem. C*, vol. 123, no. 12, pp. 7045–7053, Mar. 2019.

[33] J. G. Simmons and M. C. Tam, "Theory of isothermal currents and the direct determination of trap parameters in semiconductors and insulators containing arbitrary trap distributions," *Phys. Rev. B, Condens. Matter*, vol. 7, no. 8, pp. 3706–3713, Apr. 1973.

[34] J. G. Simmons and G. W. Taylor, "High-field isothermal currents and thermally stimulated currents in insulators having discrete trapping levels," *Phys. Rev. B, Condens. Matter*, vol. 5, no. 4, pp. 1619–1629, Feb. 1972.

[35] J. Li, F. Zhou, D. Min, S. Li, and R. Xia, "The energy distribution of trapped charges in polymers based on isothermal surface potential decay model," *IEEE Trans. Dielectr. Electr. Insul.*, vol. 22, no. 3, pp. 1723–1732, Jun. 2015.

[36] B. X. Du, Z. R. Yang, Z. L. Li, and J. Li, "Temperature-dependent nonlinear conductivity and carrier mobility of silicone rubber/SiC composites," *IEEE Trans. Dielectr. Electr. Insul.*, vol. 25, no. 3, pp. 1080–1087, Jun. 2018.

[37] Y. Zhang, L. Zhang, Y. Zhou, M. Chen, Z. Zhou, J. Liu, and Z. Chen, "DC electrical tree initiation in silicone rubber under temperature gradient," *IEEE Trans. Dielectr. Electr. Insul.*, vol. 25, no. 3, pp. 1142–1150, Jun. 2018.

[38] S. L. Roy, P. Segur, G. Teyssedre, and C. Laurent, "Description of bipolar charge transport in polyethylene using a fluid model with a constant mobility: Model prediction," *J. Phys. D, Appl. Phys.*, vol. 37, no. 2, pp. 298–305, Jan. 2004.

[39] N. Shimizu, K. Uchida, and S. Rasikawan, "Electrical tree and deteriorated region in polyethylene," *IEEE Trans. Electr. Insul.*, vol. 27, no. 3, pp. 513–518, Jun. 1992.

[40] X. Chen, Y. Xu, and X. Cao, "Nonlinear time series analysis of partial discharges in electrical trees of XLPE cable insulation samples," *IEEE Trans. Dielectr. Electr. Insul.*, vol. 21, no. 4, pp. 1455–1461, Aug. 2014.

[41] T. Han, B. Du, T. Ma, F. Wang, Y. Gao, Z. Lei, and C. Li, "Electrical tree in HTV silicone rubber with temperature gradient under repetitive pulse voltage," *IEEE Access*, vol. 7, pp. 41250–41260, 2019.

[42] B. X. Du, J. Li, and Y. Sekii, "Effects of ZnO particles on space charge of EVA copolymer for HVDC cable accessory insulation," *IEEE Trans. Dielectr. Electr. Insul.*, vol. 24, no. 3, pp. 1503–1510, Jun. 2017.

[43] X. Chen, Y. Xu, X. Cao, and S. M. Gubanski, "Electrical treeing behavior at high temperature in XLPE cable insulation samples," *IEEE Trans. Dielectr. Electr. Insul.*, vol. 22, no. 5, pp. 2841–2851, Oct. 2015.

[44] T. Tanaka, "Charge transfer and tree initiation in polyethylene subjected to AC voltage stress," *IEEE Trans. Electr. Insul.*, vol. 27, no. 3, pp. 424–431, Jun. 1992.

BOXUE DU (Senior Member, IEEE) is currently a Professor and the Director-Founder of the Institute of High Voltage, School of Electrical and Information Engineering, Tianjin University, China. His research interests are focused on dielectric failure mechanisms of polymer insulating materials, electrical insulation technology, and application of polymer dielectrics under various extreme environments, such as cryogenic, high temperature, high altitude, gamma-ray irradiation, and high-intensity magnetic field. He has published five books and nine book chapters in polymer dielectrics, and has authored about 500 articles and over 150 of them published in the IEEE TRANSACTIONS. He has also served in industry and start-ups, as a consultant. He is an Editorial Boards Member of *High Voltage*, the *Journal of Modern Power Systems and Clean Energy*, the *Chinese Journal of High Voltage Engineering*, *Insulation Materials*, and *Electrical Engineering*. He is a Fellow of IET and a member of several WG in CIGRE. He has served as an Associate Editor for the IEEE TRANSACTIONS ON DIELECTRICS AND ELECTRICAL INSULATION, for about ten years. He is an Associate Editor of IEEE ACCESS and *IET Nanodielectrics*.

TINGTING MA was born in Hebei, China, in 1992. She received the B.Eng. degree in electrical engineering in 2017. She is currently pursuing the M.Eng. degree in electrical engineering with Tianjin University. Her research interest includes the growth characteristics of electrical trees in cable insulation material and partial discharge detection.

JINGANG SU (Member, IEEE) was born in Hebei, China, in 1988. He received the Ph.D. degree in high voltage and insulation technology from the School of Electrical and Information Engineering, Tianjin University, in 2019. He is currently engaged in research on the aging problem of EPDM. His main research interests include the partial discharge phenomena and detection methods of polymer insulating materials in power cables.

MENG TIAN was born in Hubei, China, in 1995. He received the B.Eng. degree from Tianjin University, where he is currently pursuing the M.Sc. degree in high voltage engineering and automation. He is currently engaged in research on the electrical tree aging problem of epoxy resin. His main research interests include the breakdown phenomena of polymer insulating materials and space charges analysis in polymers.

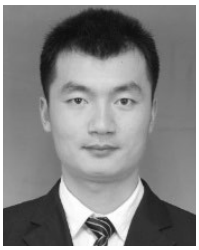

TAO HAN (Member, IEEE) was born in Shandong, China. He received the M.E. and Ph.D. degrees in electrical engineering from Tianjin University, China, in 2012 and 2015, respectively. Since 2015, he has been a Lecturer with the School of Electrical Engineering and Automation, Tianjin University, China. He is currently a Visiting Scholar at the Department of Electrical Engineering, University of Bologna, Bologna. His main research interests are degradation of cable insulation and partial discharge detection.

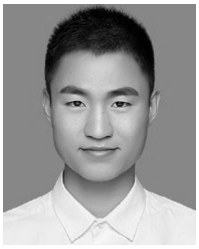

XIAOXIAO KONG was born in Liulin, China, in 1993. He received the B.S. degree in electrical engineering from Tianjin University, China, in 2015. He is currently pursuing the Ph.D. degree with the School of Electrical Engineering and Automation, Tianjin University. His main research interest is insulation design of condenser core of dry bushing, and dielectric properties of epoxy resin and its composites.